



Branch biomass allometries for urban tree species based on terrestrial laser scanning (TLS) data

Leila Parhizgar¹ · Nayanesh Pattnaik¹ · Hadi Yazdi² · Shu Qiguan² · Stephan Pauleit¹ · Mohammad A. Rahman³ · Ferdinand Ludwig² · Hans Pretzsch^{4,5} · Thomas Rötzer¹

Received: 16 October 2024 / Accepted: 21 May 2025
© The Author(s) 2025

Abstract

Key message Developed species-specific allometric equations using terrestrial laser scanning (TLS). Found significant species-specific differences in branch biomass allocation. Introduced a non-destructive method for estimating urban tree biomass.

Abstract Urban trees contribute to climate change adaptation by providing multiple ecosystem services, including carbon sequestration. Yet accurate information about above-ground biomass, particularly branch biomass, is scarce. This study aimed to develop allometric models for estimating branch biomass for ten common European urban tree species using terrestrial laser scanning (TLS) and quantitative structure models (QSM) data. Conducted in Munich, the study analyzed 3,283 trees, using structural variables such as diameter at breast height (dbh), height, and crown diameter. The dbh of trees in the dataset reached up to 0.8 m, with mean above-ground biomass ranging from 550 to 1.496 kg C, and branch biomass from 32.2 to 164.5 kg C. The results confirmed that dbh was the strongest predictor of branch biomass ($r=0.69-0.9$), and adding height improved model accuracy ($R^2=0.69-0.93$). Species-specific models revealed significant variations, with *R. pseudoacacia* showing the highest branch biomass when standardized by tree height, and *P. nigra 'italica'* the lowest. Conversely, when standardized by dbh, *P. acerifolia* showed the highest branch biomass and *C. betulus* the lowest. Comparisons with established forest tree models revealed that the developed allometric models tend to underestimate branch biomass for most species, with deviations ranging from 1 to 36%, reflecting unique growth forms and urban environmental conditions. The study highlights the need for species-specific allometric models to improve assessments of ecosystem services provided by urban trees.

Keywords Urban Trees · Branch Biomass · TLS · Allometric Relationships · QSM · TreeML-Data

Introduction

Urban trees are crucial for ecosystem services, with their size and structure directly influencing urban forest functionality and associated economic, social, and ecological benefits (Chave et al. 2014; Forrester et al. 2017; Henry et al.

Communicated by Locosselli.

✉ Leila Parhizgar
leila.parhizgar@tum.de

✉ Nayanesh Pattnaik
nayanesh.pattnaik@tum.de

¹ Strategic Landscape Planning and Management, TUM School of Life Sciences, Technical University of Munich, Emil-Ramann-Str. 6, 85354 Freising, Germany

² Green Technologies in Landscape Architecture, School of Engineering and Design, Technical University of Munich, Emil-Ramann-Str. 6, 85354 Freising, Germany

³ School of Agriculture, Food and Ecosystem Sciences, The University of Melbourne, Burnley, VIC 3121, Australia

⁴ Tree Growth and Wood Physiology, TUM School of Life Sciences, Technical University of Munich, Hans-Carl-von-Carlowitz-Platz 2, Freising 85354, Germany

⁵ SMART Ecosystems Research Group, Department of Plant Production and Forest Resources, University Institute of Research in Sustainable Forest Management (iuFOR), Associated R+D+I Unit of CSIC, Higher Technical School of Agricultural Engineering of Palencia, University of Valladolid, Avda. de Madrid 44, 34004, Palencia, Spain

2013; Paul et al. 2016; McPherson et al. 2016; Stoffberg et al. 2010; Xiao et al. 2000). Accurate quantification of above-ground biomass (AGB) is essential for evaluating carbon storage and understanding the full range of ecosystem services (ESS) provided by urban forests (Arseniou et al. 2023; Baker et al. 2019; Casalegno et al. 2017; Nowak and Greenfield 2020; Phillips et al. 2019). On the other hand, below-ground biomass (BGB) is also an important parameter in understanding total tree function and ESS. However, studies showed that BGB responses to diversity are frequently weak or inconsistent, making AGB a more robust and representative metric for productivity and ESS assessment (Martin-Guay et al. 2020). Further, measuring below-ground biomass (BGB) requires different methods and is difficult to measure in urban environments due to built infrastructure and safety reasons. Tree AGB can be directly measured by weighing tree components (i.e., branches, stems and leaves) and quantifying the moisture of green biomass after a tree has been harvested (Arseniou et al. 2023; Burt et al. 2019; Kükenbrink et al. 2021). However, this method is time-consuming and costly, and only a limited number of trees can be destructively sampled in urban areas (Calders et al. 2015; Weiskittel et al. 2015). Therefore, the total AGB of trees and their biomass components (mass of branches, main stem and leaves) are usually estimated indirectly with allometric models—statistical models defining relationships between tree biomass and commonly measured tree variables e.g., diameter at breast height (dbh), tree height, and crown dimensions (Dettmann and MacFarlane 2019; MacFarlane 2010, 2015; Radtke et al. 2017; Ver Planck and MacFarlane 2014, 2015). The abbreviations of technical terms used in this paper are summarized in the glossary provided in the supplementary section (see Table S1).

While allometric equations are widely used in forest mensuration, their application to urban trees are complicated by distinct growth patterns mainly due to heterogeneity in urban growth conditions and biomass distributions not found in forest settings (Anderegg et al. 2015; López-López et al. 2017; Peper and McPherson 1998). Urban trees exhibit distinct growth patterns and biomass distribution across their stem, branches and leaves. For example, tree crowns in forests often compete for limited space and may not reach their full expansion potential (Martin et al. 2016). Consequently, the development of allometric equations modified to urban open-grown trees has been inconsistent (McHale et al. 2009).

In recent years, landscape architects and planners have become increasingly dependent on three-dimensional (3D) models to envision diverse landscapes using allometric equations for tree growth modelling (Larsen and Kristoffersen 2002). Recent advancements in terrestrial laser scanning (TLS) have revolutionized the field of non-destructive biomass estimation. TLS enables precise measurements of tree

architecture, providing valuable data for developing accurate allometric models (Barbeito et al. 2017; Calders et al. 2015; Stovall et al. 2018). The integration of Quantitative Structure Models (QSM) with TLS data, as explored by Raumonon et al. (2013) further enhances the ability to estimate biomass, particularly in urban environments where traditional methods face limitations. The essence of trees' QSMs are detailed geometrical and topological woody tree segments above the ground (Åkerblom et al. 2017). They reconstruct dense point clouds to cylinders to inspire the further potential of the data in describing an overall branching pattern (i.e., towards zenith angle) and the length, radius, and volume for every single branch segment. Multiple methods to construct QSMs were invented over a decade, including SkelTre (Bucksch et al. 2010), treeQSM (Ramonon et al. 2013), PyTree (Delagrangé et al. 2014), simpleTree (Hackenberg et al. 2015), 3D forest (Trochta et al. 2017), AdTree (Du et al. 2019) and AdQSM (Fan et al. 2020). In recent years, TreePartNet applied a neural network in this process (Liu et al. 2021). However, previous studies were developed from limited datasets that may exhibit bias across various species and environmental conditions (López-López et al. 2017). And lower precision is expected in describing the fine ends of branches. Nevertheless, the convergence of high-resolution remote sensing and TLS technologies offers a promising solution for mapping and quantifying individual trees in urban landscapes (Roman et al. 2017; Seiferling et al. 2017; Erker et al. 2019; Parmehr et al. 2016; Ucar et al. 2018). TLS provides a non-destructive approach for quantifying tree architecture and dimensional properties (e.g., woody volume), which can be converted to AGB estimates (Calders et al. 2015; Disney et al. 2018; Kaasalainen et al. 2014).

This advancement has been increasingly applied in forest surveys, allowing remote sensing specialists to capture detailed tree structures. For example, TLS has been used to assess crown characteristics (Barbeito et al. 2017), describe crown displacement (Seidel et al. 2011), and analyze crown profiles (Ferrarese et al. 2015). It has also been applied to measure crown volume and surface area (Fernández-Sarría et al. 2013; Metz et al. 2013), branch angles (Bayer et al. 2013), and to map stem and branch topologies (Lau et al. 2018; Tarsha Kurdi et al. 2024). However, there relatively a few studies utilizing TLS for AGB estimation in urban environments (e.g., D'hont et al. 2024; Fernández-Sarría et al. 2013; Kükenbrink et al. 2021); ; , Wilkes et al. 2018, Wu et al. 2022). These studies have consistently demonstrated the high accuracy and potential of the TLS method for non-destructive biomass quantification in complex urban settings.

Nevertheless, despite the advancements in QSM techniques and the application of allometric equations, the accuracy of branch biomass estimation using the QSM data derived from TLS remains insufficiently explored for

urban tree contexts. Therefore, the aim of this study was to develop a non-destructive branch biomass model based on allometric relationships for ten European abundant tree species by utilizing the TLS and QSM data. We aim to answer the following questions:

Q-1: Can species-specific allometric equations be developed to estimate branch biomass using Quantitative Structure Model (QSM) data derived from Terrestrial Laser Scanning (TLS)?

Q-2: Are there significant differences in the relationship between tree structural dimensions (dbh, height, and crown diameter) and branch biomass among different tree species?

Q-3: Do the allometric relationships observed in urban trees differ significantly from those found in previous studies based on forest-grown trees?

Materials and methods

Material (TreeML-Data)

In this study, we employed the open-access TreeML-Data dataset (Yazdi et al. 2024) for model development. This dataset includes 3,283 point clouds of trees from public green spaces in Munich, which is the third largest city in Germany, with a population of 1.6 million (LH München 2023). Munich has a temperate climate with warm summers, and the close proximity to the Alps influences its climate. Munich boasts a wide variety of tree species that can enhance the diversity of our urban tree dataset for model development. Based on our knowledge, TreeML-Data is the only open-source QSM dataset available for urban trees. Consequently, we utilized this dataset as the primary resource for our study.

TreeML-Data comprises dbh, tree height, and crown diameter. This data was used as the primary material for our model development. Besides, QSMs, as detailed tree structure measurements and tree graph structure models relevant to these urban trees, were also included in TreeML-Data. The QSMs were originally obtained from point clouds for individual trees. TreeQSM Raunonen et al. (2013) was programmed in MATLAB (The MathWorks Inc., 2024) and used for extracting their QSMs. They consist of cylinders, including their IDs, the coordinates of their starting points, axis directions, length, and radius. They also contain the IDs about which branch they belong to, the hierarchical order of this branch, their sequences in this branch, and ID pointers about their parent cylinders and child cylinders. Figure 1 shows an example tree from TreeML-Data in two data formats: point cloud (left) and QSM data (right). The QSM data was

analyzed to extract detailed information on tree structure, branch biomass, and woody volume.

For this study, we focus on the ten most frequently occurring species from the TreeML-Data dataset. These are common species in European cities with a temperate climate (Weller 2021). The species are: *Aesculus hippocastanum*, *Acer platanoides*, *Acer pseudoplatanus*, *Carpinus betulus*, *Corylus colurna*, *Fraxinus excelsior*, *Platanus x acerifolia*, *Populus nigra var. 'Italica'*, *Robinia pseudoacacia*, and *Tilia cordata*. In total, our analysis considers 3,283 trees in public open spaces such as streets and squares. An overview of the key characteristics of these ten tree species and the structure of the dataset is indicated in Table 1.

Data preprocessing

Separating branch and stem

Based on the presented QSM data, we retrieved the height to the crown (hcb) base as follows. Firstly, we selected all branches whose hierarchical orders are larger than 0, excluding the tree stem. Then, the lowest height of their branch start was taken as the height to the crown base (see “hcb” in Fig. 2). All the cylinders that started above the hcb were labelled as branches, while the cylinders below this height were recognized as the stem (see green and red in Fig. 1 right). Enquist et al. (1998) or Niklas and Enquist (2001) define the stem as stretched from the ground to the highest tip of a tree. However, since such a stretched stem is not clearly recognizable for all tree species, we have favored the above approach. With our defined category of the branch and stem, we summed up their cylinder volumes by Eq. (1), where r and l are the radius and length of the labelled cylinders of branches or the stem, respectively.

$$V = \sum_{i=1}^n \pi r_i^2 \cdot l_i \quad (1)$$

Branch volume to biomass

The total woody volume of branches and the stem computed from the previous step was converted to biomass by multiplying the volumes by the corresponding wood density values using Eq. (2). This equation is applied to both branch biomass and stem biomass calculations.

$$B = V * \rho_{\text{species}} * \text{carbon fraction} \quad (2)$$

With B : biomass [kg C], V : volume [m³] and ρ_{species} : wood density [m³ kg⁻³] of the tree species (see Table 2),

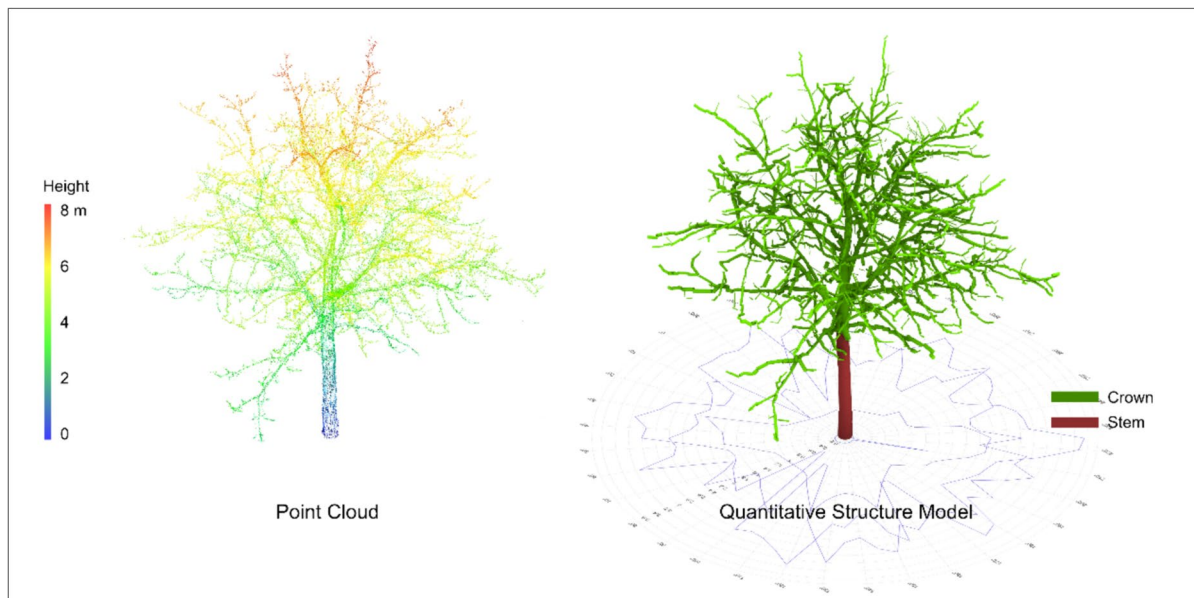


Fig. 1 A sample tree in TreeML-Data in different data formats. Left is the point cloud used for extracting structural measurements. The right image is a visualization of the QSM data, which is divided into the stem and the crown by the height of the starting point of the lowest branch

Table 1 Mean (minimum/maximum) characteristics of the different tree species in the TreeML-Data

Species	Common name	n	dbh [m]	Height [m]	Crown diameter [m]
<i>A. hippocastanum</i>	Horse chestnut	256	0.45 (0.06/0.93)	14.9 (4.8/22.2)	10.5 (1.6/18.9)
<i>A. platanoides</i>	Norway maple	716	0.33 (0.07/0.89)	13.5 (5.3/23.4)	9.1 (2.3/21.8)
<i>A. pseudoplatanus</i>	Sycamore maple	29	0.37 (0.1/0.8)	14.3 (6.7/21.9)	9.4 (2.7/16.4)
<i>C. betulus</i>	Hornbeam	31	0.24 (0.08/0.45)	11.8 (6.2/18.0)	7.4 (2.4/14.3)
<i>C. colurna</i>	Turkish hazel	77	0.23 (0.08/0.39)	10.5 (5.6/15)	6.6 (2.6/9.9)
<i>F. excelsior</i>	Common ash	79	0.34 (0.065/0.84)	13.6 (5.5/21)	8.8 (1.9/14.4)
<i>P. x acerifolia</i>	London plane	509	0.41 (0.08/0.76)	18.3 (7.9/26.1)	13.4 (4.0/22.5)
<i>P. nigra</i> 'Italica'	Lombardy poplar	275	0.46 (0.08/0.95)	24.0 (8.08/31.9)	4.2 (0.1/8.03)
<i>R. pseudoacacia</i>	Black locust	495	0.33 (0.07/0.87)	12.9 (3.9/22.5)	9.1 (2.3/21.0)
<i>T. cordata</i>	Small leaved lime	816	0.35 (0.06/0.77)	15.2 (5.2/27.7)	9.9 (2.5/17.1)

and carbon fraction is 0.5 (Cánovas et al. 2021; Matthews 1993). To estimate branch biomass for the selected tree species, wood density estimates were gathered from multiple studies and applied to individual tree volume measurements (see Table 2). The combination of Tables 1 and 2 shows diversity in structural and ecological functions of the tree samples within the study area. For instance, *P. nigra* 'Italica'

exhibited the highest average height (24.0 m) and crown diameter variability, despite having one of the lower wood densities (450 kg m^{-3}). *C. betulus* stood out with the highest wood density (750 kg m^{-3}) but displayed relatively smaller dimensions in terms of dbh and height. *A. hippocastanum*, with a wood density of 525 kg m^{-3} . *P. x acerifolia* is notable for its maximum height of 26.1 m.

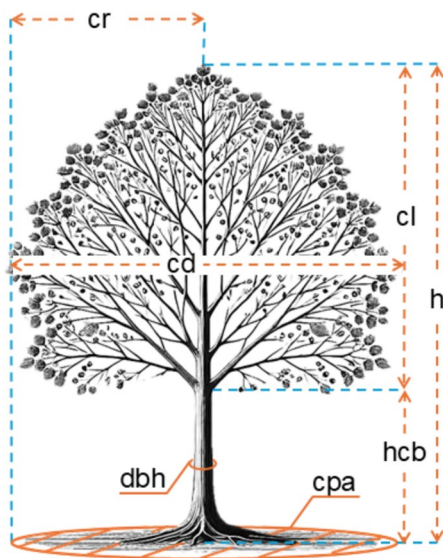


Fig. 2 Visualization of variables used in this study for quantifying tree structure and crown morphology. dbh stem diameter at height 1.3 m, h tree height, hcb height to crown base, cl crown length, cr crown radius, cd crown diameter, cpa crown projection area

Table 2 Wood density of tree species (based on Rötzer et al. 2019, derived from Cienciala et al. 2005; McPherson et al. 2016; Merganič et al. 2017)

Species	Common name	Wood density [kg m ⁻³]
<i>A. hippocastanum</i>	Horse chestnut	525
<i>A. platanoides</i>	Norway maple	565
<i>A. pseudoplatanus</i>	Sycamore maple	547
<i>C. betulus</i>	European hornbeam	750
<i>C. colurna</i>	Turkish hazel	615
<i>F. excelsior</i>	Common ash	610
<i>P. x acerifolia</i>	London plane	548
<i>P. nigra</i> ‘Italica’	Lombardy poplar	450
<i>R. pseudoacacia</i>	Black locust	691
<i>T. cordata</i>	Small-leaved lime	456

Data cleaning

TreeML-Data used point cloud data to generate the Quantitative Structure Models (QSM) of each tree. However, acquiring the point cloud data by TLS is not immune to errors, which can arise from various factors such as noise, instable surfaces, or invalid objects in reflections. These errors can propagate into QSM, leading to inaccuracies in key measurements such as dbh, tree height, or crown diameter. As a result, the final dataset can include outliers and anomalies that, if left unaddressed, could significantly affect the integrity of the analysis.

To prepare a cleaned dataset for analysis, we conducted a thorough data-cleaning process, which is a crucial step to ensure the quality and reliability of the results. Data cleaning is essential because it helps to eliminate inaccuracies, inconsistencies, and irrelevant information that could distort the findings. In our case, outliers in measurements such as dbh or crown length (see “cl” in Fig. 2) needed to be identified and corrected or removed. For instance, trees with a dbh exceeding 0.8 m were excluded, as larger trees tend to introduce greater uncertainties and errors in TLS measurements, as noted by Calders et al. (2015). These larger trees are prone to measurement inaccuracies due to the limitations of the QSM model in capturing the full complexity of their structure.

Allometry equations

Allometry is used to analyze and predict the relationship between a component of tree biomass (root, stem, branch or foliage) from readily measurable tree dimensions (for e.g., dbh or tree height). Allometric relationships are mathematically expressed through allometric equations, and the approach typically involves logarithmically transforming the size variables and then applying regression analysis to the transformed data (Pretzsch 2010). From this, we estimated allometric factors and exponents. In this study, for each species, the relationship between several tree structural parameters and branch biomass were evaluated. The examined relationships were between branch biomass and various tree dimensions, including dbh, height (h), crown projection area (cpa), and crown diameter (cd). As cpa and cd were highly correlated, we included only cd for further analysis. In the first step, graphical exploration through scatter plots yielded visual relations between the variables and gave an idea of the model to be fitted (for e.g., linear vs. log models). Then, species-specific branch biomass allometry was developed using power equations in two main categories: First, single effect models, which analyzed the relation of dbh (Eq. 3), h (Eq. 4), or cd (Eq. 5) as single variables with the branch biomass (BB). Second, double effect models, in which two variables were paired for the analysis: namely dbh and h (Eq. 6), h and cd (Eq. 7), and dbh and cd (Eq. 8). The models were then further checked to meet the requirements of heteroskedasticity (Picard et al. 2012). Ordinary least squares (OLS) regressions were used on the log-transformed variables across all branch biomass equations to determine the scaling coefficient and the intercept, in the forms:

$$\ln(BB_i) = \beta_0 + \beta_i * \ln(\text{dbh}) + \epsilon_i \tag{3}$$

$$\ln(BB_i) = \beta_0 + \beta_i * \ln(h) + \epsilon_i \tag{4}$$

$$\ln(\text{BB}_i) = \beta_0 + \beta_i * \ln(\text{cd}) + \varepsilon_i \quad (5)$$

$$\ln(\text{BB}_i) = \beta_0 + \beta_{i1} * \ln(\text{dbh}) + \beta_{i2} * \ln(h) + \varepsilon_i \quad (6)$$

$$\ln(\text{BB}_i) = \beta_0 + \beta_{i1} * \ln(h) + \beta_{i2} * \ln(\text{cd}) + \varepsilon_i \quad (7)$$

$$\ln(\text{BB}_i) = \beta_0 + \beta_{i1} * \ln(\text{dbh}) + \beta_{i2} * \ln(\text{cd}) + \varepsilon_i \quad (8)$$

where BB = branch biomass, β_0 = intercept of the regression, β_{i1} and β_{i2} are the slopes of the regression and ε_i is the residual error. Regression models employing logarithmic transformations are known to produce biased biomass estimates (Montagu et al. 2005). To address this issue, we implemented a bias correction method when back-transforming our linear models. We calculated a correction factor (CF) using the mean square error (MSE) which was calculated by the equation (Baskerville 1972):

$$\text{CF} = \exp(\text{MSE}^2/2) \quad (9)$$

where MSE is the standard error of residuals obtained from the regression procedure. This CF is then multiplied to the estimates from the regression equations, yielding the final estimates for branch biomass. The selection of the best model for each species was based on the Akaike information criterion (AIC), with a lower AIC indicating a better model fit. We complemented AIC along with additional metrics, including root mean square error (RMSE) to quantify prediction accuracy, and the coefficient of determination (R^2) to assess the proportion of variance explained by each model. To ensure the robustness of our model selection, we also evaluated model assumptions. The normality of residuals was assessed using visual inspection (Q–Q plots). Homoscedasticity was examined through residual plots against fitted values and predictor variables.

Comparison of allometric estimates with established models

Allometric models developed from our TLS data were directly compared to existing models from the literature. A tree-level comparison was used to assess the performance of our branch biomass allometric models compared to existing equations from literature. Given the scarcity of urban-specific branch biomass estimates and models, we could only use the estimates derived from forest trees and identified comparable models for five (*A. pseudoplatanus*, *C. betulus*, *F. excelsior*, *R. pseudoacacia*, *T. cordata*) of our ten studied species. We compared the branch biomass estimates from Forrester et al. (2017) for *A. pseudoplatanus*, *C. betulus*, *F. excelsior*, *R. pseudoacacia* and *T. cordata* from Čihák et al. (2014). Absolute and relative RMSE were used to evaluate

all the models. Bias, which would account for systematic over- or under-estimation, was calculated as through Eq. (10) as follows:

$$\text{Bias} = \frac{\sum_{i=1}^n (y_i - \hat{y}_i)}{n} \quad (10)$$

where y_i is the i th estimate of branch biomass for an individual tree. The reference studies and their corresponding values are detailed in Supplementary Table S2. All analyses were carried out using functions and packages in the statistical software R (R Core Team 2024).

Results

Branch and total biomass distribution across tree species

To answer the first research question, we first calculated the total and branch biomass across the ten different species (Table 3). We found significant variations across the tree species. Here, the wood density values represent whole tree density rather than specific tree components (stem density or branch density). In terms of total biomass, there was a wide variation both between and within species (i.e., tree size). *P. x acerifolia* with a mean dbh of 0.41 m exhibited the highest mean per-individual aboveground-tree biomass (1496.4 kg C), while *C. colurna* with a mean dbh of 0.23 m had the lowest (550.9 kg C). Branch biomass showed a similar trend of variation. *P. nigra* ‘Italica’ had the highest mean branch biomass (164.5 kg C), closely followed by *P. x acerifolia* (154.9 kg C) and *A. hippocastanum* (153.1 kg C). In contrast, *C. betulus* showed the lowest mean branch biomass (32.2 kg C). The last column of Table 3 represents percentage of branch biomass relative to total biomass. *P. nigra* ‘Italica’ had the highest share (17.9%), followed by *F. excelsior* (15.7%) and *A. hippocastanum* (12.3%). On the other hand, *C. betulus* had the lowest branch share at 3.4%, with *A. pseudoplatanus* and *T. cordata* also showed relatively lower shares at 8.8% and 7.1%, respectively.

Species-specific branch biomass predictions depending on tree structural dimensions

As the second objective of this study, we established various models to find the allometry relations between tree branch biomass and tree structural dimensions. Larger trees tended to have higher branch biomass, but the degree of variability also increased with tree size for most species (Fig. 3). Figure 3a depicts the relationship between branch biomass and dbh: *P. nigra* ‘Italica’ showed the strongest positive correlation ($r=0.91$), followed by *C. colurna* ($r=0.90$), *A.*

Table 3 Calculated total and branch biomass (mean \pm standard error) for tree species

Tree species	Wood density [kg m ⁻³]	Total biomass [kg C]	Branch biomass [kg C]	Branch/total biomass [%]
<i>A. hippocastanum</i>	525	1241.8 \pm 50.9	153.1 \pm 6.8	12.3 \pm 1.05
<i>A. platanoides</i>	565	879.5 \pm 26.6	98.3 \pm 3.1	11.2 \pm 0.69
<i>A. pseudoplatanus</i>	547	957.2 \pm 130.4	84.5 \pm 13.1	8.8 \pm 2.62
<i>C. betulus</i>	750	945.2 \pm 110.8	32.2 \pm 3.8	3.4 \pm 0.81
<i>C. colurna</i>	615	550.9 \pm 43.3	39.7 \pm 3.0	7.2 \pm 1.12
<i>F. excelsior</i>	610	727.6 \pm 52.7	114.3 \pm 9.8	15.7 \pm 2.50
<i>P. x acerifolia</i>	548	1496.4 \pm 36.7	154.9 \pm 3.1	10.4 \pm 0.46
<i>P. nigra</i> 'Italica'	450	921 \pm 32.1	164.5 \pm 3.2	17.9 \pm 0.97
<i>R. pseudoacacia</i>	691	1253.3 \pm 43.9	125.6 \pm 4.2	10.0 \pm 0.69
<i>T. cordata</i>	456	1313.5 \pm 26.9	93.1 \pm 1.9	7.1 \pm 0.29

hippocastanum ($r=0.82$), *A. platanoides* ($r=0.77$), and *P. x acerifolia* ($r=0.77$). The weakest, yet still significant, correlation was observed in *F. excelsior* ($r=0.69$). Figure 3b presents the relationship between branch biomass and height, in which most species fell within the range of $r=0.70$ – 0.76 , indicating a consistent strong correlation between height and branch biomass. Similar to dbh, *P. nigra* 'Italica' showed the strongest positive correlation ($r=0.81$) with height. Although there was a significant positive correlation between crown diameter and branch biomass, they were generally lower than those for corresponding dbh and height (Fig. 3(c)). For more detailed model results see Table S2 in the supplementary sections.

To enable a standardized comparison of branch biomass across our ten tree species, we analyzed the data within a consistent height range (Fig. 4a) and branch biomass allocation relative to the dbh (Fig. 4b). The result revealed significant differences in branch biomass among species at standardized height ($F(9, 587) = 24.41, p < 0.001$) and relative to per cm dbh ($F(9, 3254) = 48.45, p < 0.001$). The mean height of the dataset with a tolerance level of $15.4 \text{ m} \pm 1.0$ was used to assess these differences. *R. pseudoacacia* showed the highest branch biomass (mean \pm SE = 175.3 ± 7.8 kg C), significantly higher than most other species except for *F. excelsior* (155.8 ± 14.1 kg C) and *A. hippocastanum* (mean = 154.9 ± 9.5 kg C). In contrast, *P. nigra* 'Italica' (32.5 ± 4.9 kg C) displayed the lowest branch biomass at the standardized height, significantly lower than all other species except for *A. pseudoplatanus* (44.8 ± 18.1 kg C). This disparity represents an approximately 80% difference in branch biomass between the highest and lowest values observed among the species studied. Standardizing branch biomass by per cm of dbh demonstrated that *P. acerifolia* had the highest branch biomass per dbh (3.62 ± 0.11 kg C/cm), significantly higher than most species except *R. pseudoacacia* (3.41 ± 0.09 kg C/cm). *C. betulus* (1.40 ± 0.05 kg C/cm) and *P. nigra* 'Italica' (1.49 ± 0.08 kg C/cm) had the lowest values, significantly lower than all species except *C.*

colurna (1.57 ± 0.13 kg C/cm). This indicates a 61% difference in branch biomass allocation per unit trunk diameter between the highest and lowest values.

Species-specific branch biomass allometric equations

To address the second research question, we developed species-specific allometric equations for estimating branch biomass. Table 4 shows all allometry equations for the global models incorporating Eqs. (3)–(8) for all ten species together. Results showed the best-predicted model included both dbh and height as predictors. All species-specific models are shown in supplementary Table S2. We further ran the same model for each tree species, and we found similar results to the global models, for most of the species (see Table 5). The best predictive model for species-specific branch biomass included both dbh and height as predictors, indicated by low AIC and high R^2 values. The exceptions were *A. pseudoplatanus* and *C. colurna*, where crown diameter and dbh model were found to be the best fit. When using a single predictor variable, dbh provided the most reliable estimates compared to height and crown diameter for all the tree species.

Discussion

In this study, we could successfully use TLS data to identify key tree structural dimensions such as dbh, h, cd. Using these detailed structural measurements, we were able to calculate branch biomass for our selected tree species. Despite our research focusing on allometric equations for branch biomass, it is also noticed that the stem biomass constituted the majority of total aboveground tree biomass, accounting for approximately 86.2% on average across all species and dbh classes (see Supplementary Fig. 1). Conversely, branch biomass represented an average of 13.8% of the aboveground

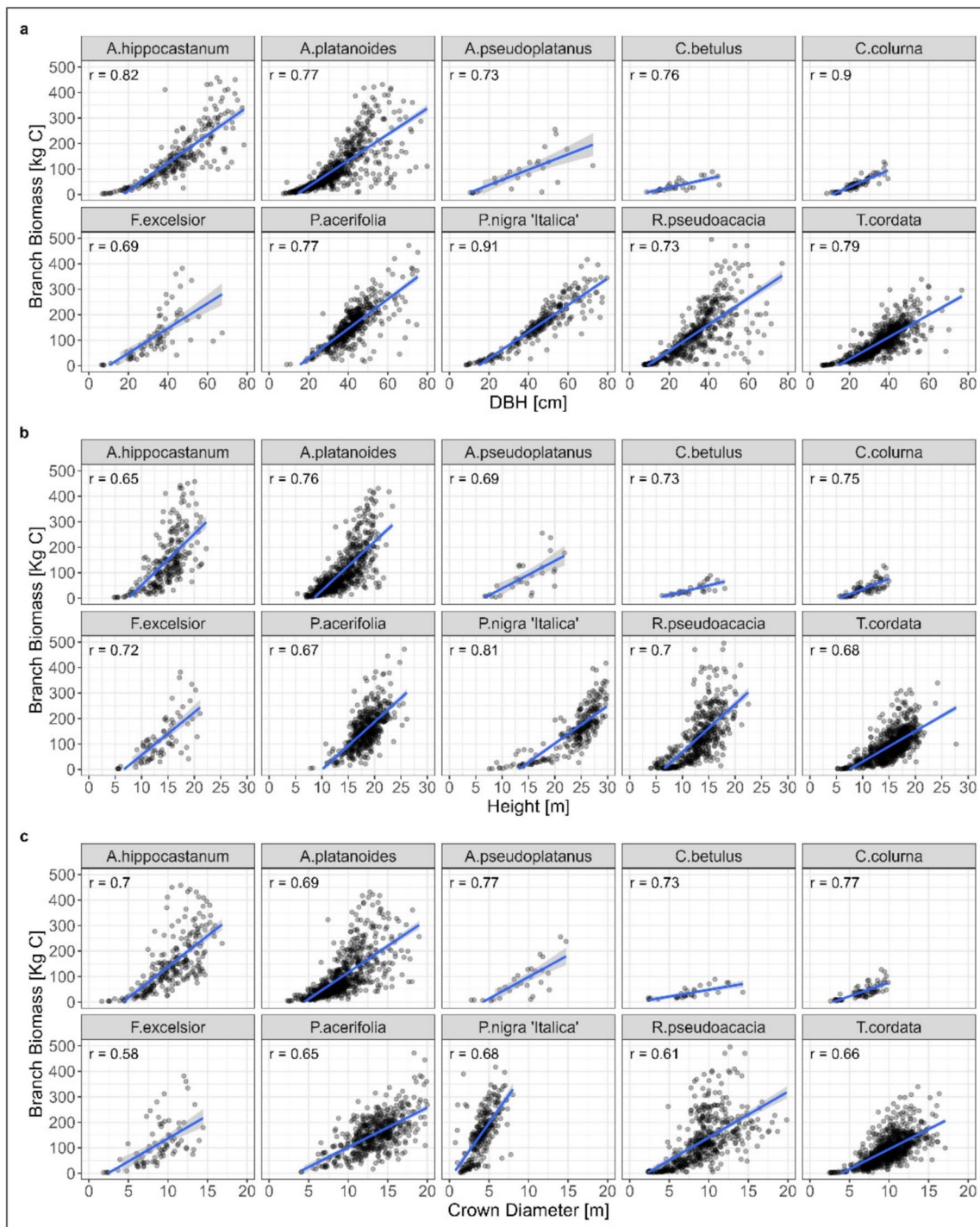


Fig. 3 Scatter plots depicting the dependency of the branch biomass to the diameter at breast height (dbh) in panel **a**, to the height in panel **b**, and to the crown diameter in panel **c** for ten tree species. “ r ” indicates the Pearson correlation coefficient

tree biomass (Figure S1). Our results highlight that branch biomass varied considerably across these most common urban tree species and was strongly affected by the structural dimensions.

Many studies have developed allometric equations to estimate branch biomass in natural forests (e.g. Vejputsková et al. 2015; Weiskittel et al. 2015; Zianis et al. 2005). Although some studies have developed similar equations for urban forests (e.g. Vaz Monteiro et al. 2016;

Fig. 4 Branch biomass across different tree species at **a** standardized height range (mean height of the dataset (15.4 m ± 1.0 m)) and **b** branch biomass per unit of dbh. The dot indicates the mean value, and the whiskers indicate the corresponding standard error. The letters on top of each error bar represent the result of the one-way ANOVA followed by post-hoc tests to assess the statistical differences among species. Means not sharing any letter are significantly different by the Tukey test at 5% level of significance. Species are arranged in descending order of mean values for each standardization method

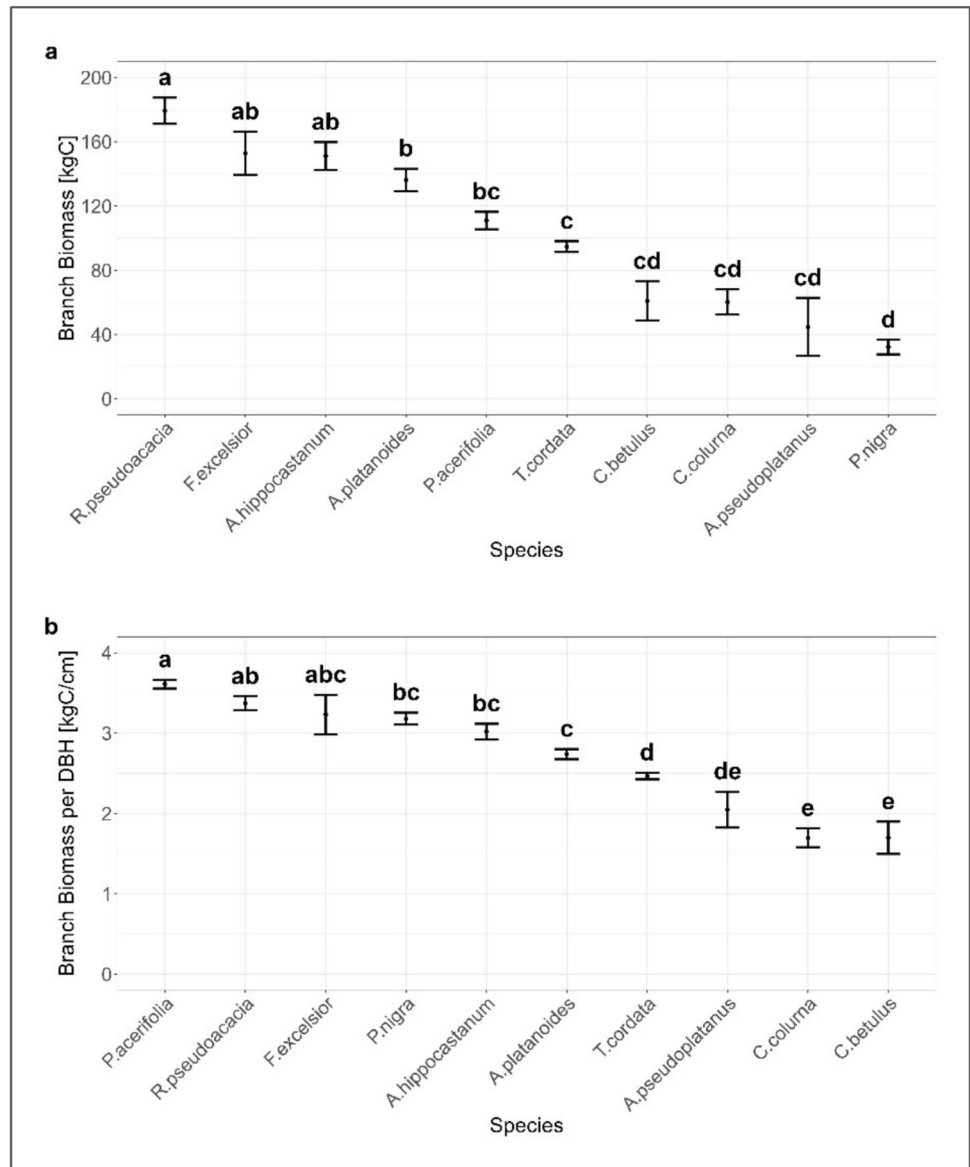


Table 4 Allometric results for all the trees species for branch biomass

Model	β_0	β_{1i}	β_{2i}	CF	AIC	R^2	P value
Equation (3)	-2.510	1.970	-	1.10	3999.5	0.77	<0.001
Equation (4)	-1.825	2.323	-	1.19	5911.4	0.59	<0.001
Equation (5)	1.678	1.263	-	1.33	7508.5	0.34	<0.001
Equation (6)	-2.992	1.564	0.71	1.09	3646.5	0.80	<0.001
Equation (7)	-2.508	1.945	0.78	1.13	4799.5	0.71	<0.001
Equation (8)	-2.502	1.857	0.18	1.10	3936.0	0.78	<0.001

Here CF is correction factor, AIC is Akaike Information Criterion

Yang et al. (2022), there are only a few studies such as Barbeito et al. (2017), Burt et al. (2021), Calders et al. (2015), Gonzalez De Tanago et al. (2018), Kükenbrink et al. (2021) and Momo Takoudjou et al. (2018) who used TLS data for deriving the branch biomass. Recent

research, for instance Demol et al. (2022), highlighted the potential of TLS to capture detailed 3D structural data that enhanced the accuracy of biomass predictions. Our study advances this field by applying TLS and QSM to develop species-specific allometric equations for urban

Table 5 Species-specific best fit allometric models for predicting branch biomass and species-specific intercepts and coefficients

Species	Model	β_0	β_{1i}	β_{2i}	CF	AIC	R^2
<i>A. hippocastanum</i>	Equation (6)	-3.423	1.763	0.581	1.056	159.98	0.887
<i>A. pseudoplatanus</i>	Equation (8)	-1.892	1.304	0.630	1.256	62.27	0.699
<i>C. betulus</i>	Equation (6)	-1.316	0.629	1.119	1.046	18.09	0.772
<i>C. colurna</i>	Equation (8)	-3.084	1.709	0.661	1.035	16.39	0.900
<i>F. excelsior</i>	Equation (6)	-3.569	1.505	1.088	1.084	82.99	0.865
<i>P. x acerifolia</i>	Equation (6)	-3.979	1.231	1.496	1.053	288.49	0.694
<i>P. nigra</i> 'Italica'	Equation (6)	-3.900	1.488	1.002	1.027	19.04	0.938
<i>R. pseudoacacia</i>	Equation (6)	-3.767	1.299	1.490	1.119	666.73	0.826
<i>T. cordata</i>	Equation (6)	-3.777	1.564	0.950	1.070	686.92	0.804

All models were statistically significant ($p < 0.001$). Here CF is correction factor, AIC is Akaike Information Criterion

trees. We developed various allometric models, and the results show heterogeneity among species related to their crown architecture and growth patterns. The following sections discuss the findings, focusing on how different structural parameters, such as dbh, h, and cd, interact to affect branch biomass across diverse urban tree species.

Branch biomass estimation depending on tree structure

The relationships between branch biomass and tree age are very valuable information, especially for planners and practitioners. However, the age of trees is difficult to determine. On the other hand, close relationships exist between tree age and dbh and tree height (Franceschi et al. 2022; Rötzer et al. 2021 or Yazdi et al. 2025). Using these equations our results can easily be converted.

Branch biomass and dbh

Our study confirmed the strong relationship between branch biomass and dbh, which emerged as the most significant predictor of tree branch biomass across the species studied. This finding is consistent with the work of Chave et al. (2014), who highlighted dbh as a critical parameter in allometric models due to its direct correlation with tree size and its role in predicting AGB. The positive correlation observed between dbh and branch biomass in species such as *P. nigra* 'Italica' ($r=0.91$) and *C. colurna* ($r=0.90$) supports the declaration by Forrester et al. (2017) that dbh is a reliable indicator of biomass across diverse species. Additionally, general allometries as proposed by Enquist et al. (1998, 1999), Niklas and Enquist (2001), Pretzsch (2009) and Weiner (2004) further support the use of dbh (tree size) as a central variable in predicting tree biomass, given its strong association with overall tree structure and resource allocation patterns. Other seven species such as *A. hippocastanum*

and *T. cordata* also showed significant correlations with dbh, with correlation coefficients of $r=0.82$ and $r=0.79$, respectively. However, variations in species-specific growth forms, such as those seen for *F. excelsior* exhibited a moderate correlation between dbh and branch biomass ($r=0.69$), indicating that factors such as branching architecture and wood density may also play significant roles in determining biomass distribution.

Branch biomass and height

Our study also identified tree height as a significant factor influencing branch biomass, with taller trees generally exhibiting more extensive and complex branching systems. Studies such as those by Burt et al. (2019) have similarly emphasized the role of height in biomass estimations, noting that taller trees can sustain larger branch systems due to enhanced resource acquisition capabilities. Our results show that species like *P. nigra* 'Italica' had the strongest correlations between height and branch biomass, with correlation coefficients of $r=0.81$. Despite the strong correlation between height and branch biomass for all ten studied tree species, the degree of effect varied among species. For instance, *A. platanoides*, *C. colurna*, *C. betulus*, *F. excelsior* and *R. pseudoacacia* showed a significant correlation between height and branch biomass ($r=0.7$). While *A. hippocastanum*, *A. pseudoplatanus*, *P. x acerifolia* and *T. cordata* exhibited a slightly lower correlation coefficient ($r=0.6$), highlighting that other factors like branching patterns and crown architecture may also play significant roles in biomass distribution for these species. Additionally, the analysis revealed that species with high wood density, such as *R. pseudoacacia* (wood density = 691 kg/m³), demonstrated robust branch biomass despite moderate height, indicating that wood density can modulate the impact of height on biomass allocation.

Branch biomass and crown diameter

While the correlation between crown diameter and branch biomass was positive, it was generally weaker than those observed with dbh and height. This finding is consistent with prior research, such as Picard et al. (2012), that suggested that crown dimensions alone may not fully capture the variability in biomass allocation due to the diverse crown shapes and branching patterns among species. However, crown diameter remains a valuable metric when combined with other variables, as it provides insights into the tree's structural characteristics and potential leaf area, which are crucial for ecological and physiological functions. Our results indicated that all the ten tree species have a moderate correlation between crown diameter and branch biomass, with correlation coefficients ranging between $r=0.7$ (*A. hippocastanum*, *A. pseudoplatanus*, *C. betulus* and *C. colurna*) and $r=0.58$ (*F. excelsior*). This may be attributed to the variability in crown architecture and branching patterns, where some species allocate more biomass to structural support rather than expanding their canopy area. These findings align with the observations by Čihák et al. (2014) and Forrester et al. (2017), who noted that species-specific growth forms and ecological strategies significantly influence the relationship between crown dimensions and biomass.

The variable correlation between crown diameter and branch biomass suggests that height, crown shape, and dbh could be added to the models to make them more accurate. The importance of crown shape in biomass distribution has been noted by Franceschi et al. (2022), and including it as a parameter might provide a more accurate representation of tree structure and biomass distribution.

Branch biomass and combined variables

Models incorporating combinations of structural variables, such as dbh and height or height and crown diameter, generally provided more accurate predictions of branch biomass than single-variable models. This combined approach accounts for the interactive effects of multiple dimensions on biomass allocation, enhancing model precision and reducing prediction errors. For example, the best predictive models for most species included both dbh and height, indicating the value of integrating these variables in allometric equations (Table 5).

Our analysis demonstrated that the use of combined variables significantly improved the accuracy of biomass estimates across several species. For instance, the model incorporating both dbh and height for *A. hippocastanum* resulted in a higher coefficient of determination ($R^2=0.88$) compared to models using dbh ($R^2=0.87$) or height ($R^2=0.68$) alone. Similarly, for *P. nigra* 'Italica', models using dbh ($R^2=0.92$) and height ($R^2=0.84$) showed improved prediction accuracy

($R^2=0.93$) compared to single variable models. The advantage of combined variable models supports findings by Forrester et al. (2017), who demonstrated that multi-variable models are more effective in capturing the complexity of biomass distribution.

Comparison with established models

As the last objective of this study, we compared our allometry results with previously established models (Čihák et al. 2014; Forrester et al. 2017). It's important to note that in our study, we did not distinguish between bark and wood when estimating the branch biomass. While wood and bark are known to have different densities, we relied specifically on wood density values from the literature for our calculations, as these were more readily available and reliable. Our results showed that the species-specific allometric equations developed for urban trees in this study revealed slight differences from those reported in earlier studies for five of the examined species (Fig. 5). It is important to note that our comparisons were with branch biomass allometric models of forest trees, which may not fully represent the varied growth conditions in urban environments. Our allometric equations tended to underestimate branch biomass in four of the five species when compared to literature-based equations, as evidenced by the negative bias values. Only *T. cordata* deviated from this pattern, showing a slight overestimation. The observed differences could be attributed to several factors. Urban trees often experience different growing conditions, including soil compaction, restricted root space, and altered light conditions, which may affect their biomass allocation patterns. While the R^2 values indicate a good fit for our models (ranging from 0.84 to 0.96), differences in sample size and dbh range between our study and the literature models could contribute to the discrepancies. Furthermore, the varying degrees of difference across species reflect species-specific responses to urban environments. The most substantial difference observed was for *A. pseudoplatanus*, where our equations differed by approximately 36% from previously published literature. *F. excelsior* also showed differences, with relative differences of 21.9% and 12.4%, respectively. *R. pseudoacacia* and *C. betulus*, exhibited more modest differences, each with a relative difference of approximately 8.5% from literature-based equations. Our allometric equations for *T. cordata* showed almost similar branch biomass estimations (relative difference ~ 1%) when compared with equations from the literature.

Novelty of the approach

Our approach of using TLS data combined with QSM methods to estimate the branch biomass of urban trees bears novelty and provides several advantages. The high-resolution

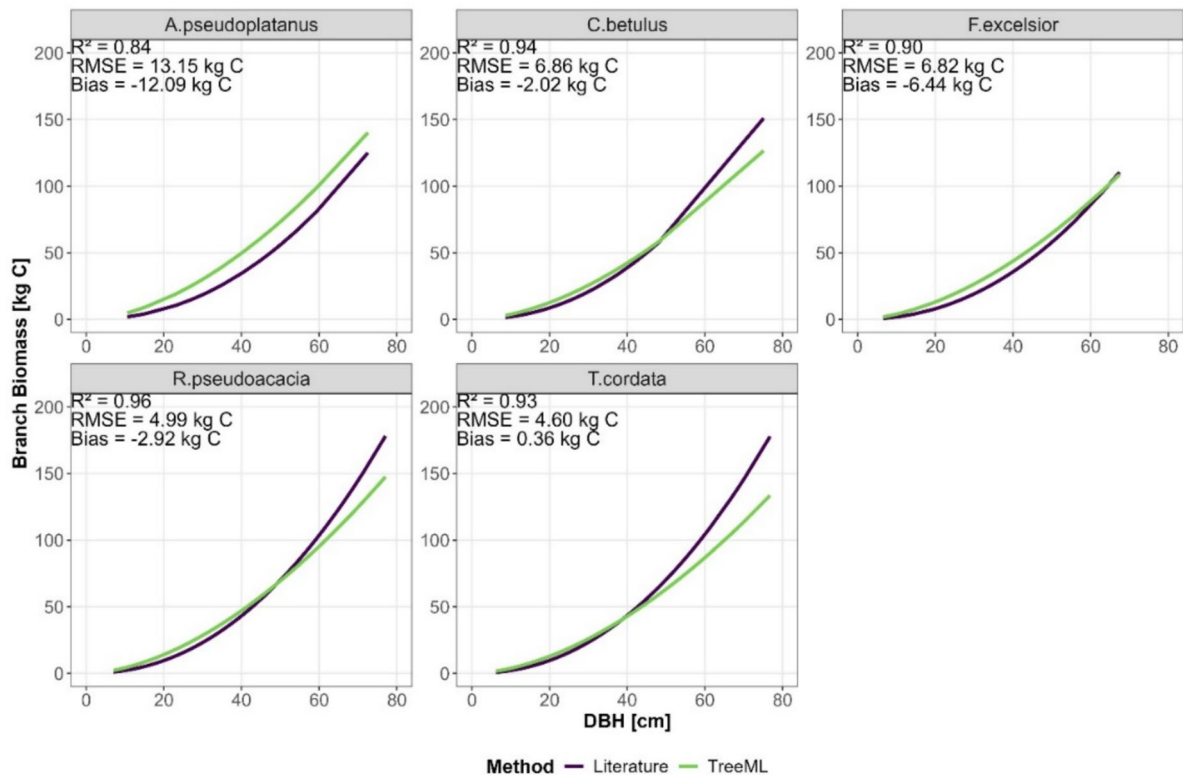


Fig. 5 Branch biomass in dependence on dbh derived allometric equations based on TreeML compared to literature sources (Čihák et al. 2014; Forrester et al. 2017))

3D data generated by TLS allows for the precise measurement of complex branching structures typical of urban trees, overcoming some limitations of traditional methods that rely on less detailed measurements. This method aligns with advancements in remote sensing technologies highlighted by Stovall et al. (2018) and Disney et al. (2018), offering a non-invasive and efficient way to estimate biomass. Furthermore, the use of QSM enables detailed structural modeling of individual branches, capturing variations in branch length, diameter, and volume, which are critical for accurate biomass estimation. Despite some limitations in precision for smaller branches, as noted by Bornand et al. (2023) and Demol et al. (2022), QSM provides a valuable tool for advancing urban forestry research and informing management practices.

Conclusion

Our study successfully developed species-specific allometric equations using TLS data, offering a non-destructive method for accurate branch biomass estimation in urban environments. Our findings reveal significant species-specific and tree dimension-specific differences in biomass allocation.

While these findings underscore the need for tailored models in urban forestry, we acknowledge certain methodological limitations. The accuracy of QSM extraction is contingent on high-quality point clouds, which were challenging to obtain for fine, distant branches. Whilst earlier research has indicated the possibility of overestimation in thin twig volumes with a diameter of less than 50 mm (Bornand et al. 2023; Demol et al. 2022), this is anticipated to exert a negligible influence on the overall crown biomass estimates derived from the majority of thicker branches.

A primary limitation lies in our validation methodology. Unlike studies utilizing destructive sampling, we lacked direct biomass measurements from urban trees. Consequently, we relied on literature-based comparisons, which may not perfectly reflect our specific urban conditions and species. The use of generalized allometric equations and wood density values derived from forest trees in literature may introduce some discrepancies. However, it is important to note that allometric equations reflect not only statistical relationships but also functional and mechanistic linkages between plant organs (e.g., hydraulics, mechanics). It is evident that there is no strict differentiation in the allometries between urban trees and forest trees; they should rather be

seen as a continuum, as solitary trees also grow in forests. For example, if competition between trees were set to zero, the allometries of urban and forest trees would certainly converge. However, other site conditions such as soil properties, mycorrhizae, radiation and/or wind conditions also have a strong impact on biomass growth and dimensional changes, thus altering the allometry of urban and forest trees in different ways.

To advance this research, we recommend expanding the study to include a broader range of species and urban environmental conditions. Additionally, focusing on urban tree stock quantification is essential, as urban forests significantly contribute to ecosystem services such as carbon sequestration. More precise biomass data will refine models, supporting better urban forest management and maximizing the environmental and climate benefits of urban green spaces.

Author contribution statement LP: Conceptualization, Formal analysis, Investigation, Methodology, Visualization, Writing—original draft, review & editing NP: Conceptualization, Formal analysis, Investigation, Methodology, Software, Visualization, Writing—original draft, review & editing HY: Data acquisition, Visualization, Writing—draft, review & editing QS: Data acquisition, Visualization, Writing—original draft, review & editing SP: Writing—review & editing, MAR: Writing—review & editing, FL: Writing—& editing, HP: Writing—review & editing, TR: Conceptualization, Methodology, Supervision, Writing—original draft, review & editing.

Supplementary Information The online version contains supplementary material available at <https://doi.org/10.1007/s00468-025-02637-7>.

Acknowledgements We thank the Deutsche Forschungsgemeinschaft (DFG) for funding the project Research Training Group Urban Green Infrastructure (Grant Number: 437788427 – RTG 2679; RTG UGI). We thank our colleagues and collaborators for their contributions. And special thanks to Dr. Astrid Moser-Reischl for her scientific support throughout this study.

Funding Open Access funding enabled and organized by Projekt DEAL. This work was carried out within the Research Training Group *Urban Green Infrastructure*, funded by the German Research Foundation (DFG) under grant 437788427 – RTG 2679. Associated with the DFG-DACH-project funds this study under No. DFG-GZ: LU2505/2-1, RO 4283/2-1 and PR 292/23-1, AOBJ:683826, 683827, and 683828 and cooperated with the DFG funded research groups under No. GRK 2678/1, AOBJ:68242, PR 292/23-1 and RO 4283/2-1.

Data Availability Statement The dataset used in this study is a subset of the openly accessible TreeML-Data, published by Yazdi et al. (2024) and available at <https://www.nature.com/articles/s41597-023-02873-x>.

Declarations

Conflict of interest The authors declare that they have no conflict of interest.

Open Access This article is licensed under a Creative Commons Attribution 4.0 International License, which permits use, sharing, adaptation, distribution and reproduction in any medium or format, as long as you give appropriate credit to the original author(s) and the source, provide a link to the Creative Commons licence, and indicate if changes were made. The images or other third party material in this article are included in the article's Creative Commons licence, unless indicated otherwise in a credit line to the material. If material is not included in the article's Creative Commons licence and your intended use is not permitted by statutory regulation or exceeds the permitted use, you will need to obtain permission directly from the copyright holder. To view a copy of this licence, visit <http://creativecommons.org/licenses/by/4.0/>.

References

- Åkerblom M, Raunonen P, Mäkipää R, Kaasalainen M (2017) Automatic tree species recognition with quantitative structure models. *Remote Sens Environ* 191:1–12. <https://doi.org/10.1016/j.rse.2016.12.002>
- Anderegg WRL, Schwalm C, Biondi F, Camarero JJ, Koch G, Litvak M, Ogle K, Shaw JD, Shevliakova E, Williams AP, Wolf A, Ziaco E, Pacala S (2015) Pervasive drought legacies in forest ecosystems and their implications for carbon cycle models. *Science* 349(6247):528–532. <https://doi.org/10.1126/science.aab1833>
- Arseniou G, MacFarlane DW, Calders K, Baker M (2023) Accuracy differences in aboveground woody biomass estimation with terrestrial laser scanning for trees in urban and rural forests and different leaf conditions. *Trees* 37(3):761–779. <https://doi.org/10.1007/s00468-022-02382-1>
- Baker ME, Schley ML, Sexton JO (2019) Impacts of expanding impervious surface on specific conductance in urbanizing streams. *Water Resour Res* 55(8):6482–6498. <https://doi.org/10.1029/2019WR025014>
- Barbeito I, Dassot M, Bayer D, Collet C, Drössler L, Löf M, Del Rio M, Ruiz-Peinado R, Forrester DI, Bravo-Oviedo A, Pretzsch H (2017) Terrestrial laser scanning reveals differences in crown structure of *Fagus sylvatica* in mixed vs. Pure European forests. *For Ecol Manag* 405:381–390. <https://doi.org/10.1016/j.foreco.2017.09.043>
- Baskerville GL (1972) Use of logarithmic regression in the estimation of plant biomass. *Can J for Res* 2(1):49–53. <https://doi.org/10.1139/x72-009>
- Bayer D, Seifert S, Pretzsch H (2013) Structural crown properties of Norway spruce (*Picea abies* [L.] Karst.) and European beech (*Fagus sylvatica* [L.]) in mixed versus pure stands revealed by terrestrial laser scanning. *Trees* 27(4):1035–1047. <https://doi.org/10.1007/s00468-013-0854-4>
- Bornand A, Rehush N, Morsdorf F, Thüring E, Abegg M (2023) Individual tree volume estimation with terrestrial laser scanning: evaluating reconstructive and allometric approaches. *Agric for Meteorol* 341:109654. <https://doi.org/10.1016/j.agrformet.2023.109654>
- Bucksch A, Lindenbergh R, Menenti M (2010) SkelTre. *Vis Comput* 26(10):1283–1300. <https://doi.org/10.1007/s00371-010-0520-4>
- Burt A, Disney M, Calders K (2019) Extracting individual trees from lidar point clouds using *treeseg*. *Methods Ecol Evol* 10(3):438–445. <https://doi.org/10.1111/2041-210X.13121>
- Burt A, Vicari MB, Coughlin I, Meir P, Rowland L, Disney M (2021) New insights into large tropical tree mass and structure from direct harvest and terrestrial lidar. *R Soc Open Sci*. <https://doi.org/10.1098/rsos.201458>
- Calders K, Newnham G, Burt A, Murphy S, Raunonen P, Herold M, Culvenor D, Avitabile V, Disney M, Armston J, Kaasalainen M

- (2015) Nondestructive estimates of above-ground biomass using terrestrial laser scanning. *Methods Ecol Evol* 6(2):198–208. <https://doi.org/10.1111/2041-210X.12301>
- Cánovas FM, Lüttge U, Risueño M-C, Pretzsch H (eds) (2021) *Progress in botany*, vol 82. Springer International Publishing. <https://doi.org/10.1007/978-3-030-68620-8>
- Casalegno S, Anderson K, Hancock S, Gaston KJ (2017) Improving models of urban greenspace: from vegetation surface cover to volumetric survey, using waveform laser scanning. *Methods Ecol Evol* 8(11):1443–1452. <https://doi.org/10.1111/2041-210X.12794>
- Chave J, Réjou-Méchain M, Búrquez A, Chidumayo E, Colgan MS, Delitti WBC, Duque A, Eid T, Fearnside PM, Goodman RC, Henry M, Martínez-Yrizar A, Mugasha WA, Muller-Landau HC, Mencuccini M, Nelson BW, Ngomanda A, Nogueira EM, Ortiz-Malavassi E, Vieilledent G (2014) Improved allometric models to estimate the aboveground biomass of tropical trees. *Glob Change Biol* 20(10):3177–3190. <https://doi.org/10.1111/gcb.12629>
- Cienciala E, Černý M, Apltauer J, Exnerová Z (2005) Biomass functions applicable to European beech. *J for Sci* 51:147–154
- Čihák T, Hlásný T, Stolariková R, Vejvustková M, Marušák R (2014) Functions for the aboveground woody biomass in Small-leaved lime (*Tilia cordata* Mill.) / Funkce pro hodnocení biomasy nadzemních částí lípy malolisté (*Tilia cordata* Mill.). For J. <https://doi.org/10.2478/forj-2014-0016>
- D'hont B, Calders K, Bartholomeus H, Lau A, Terryn L, Verhelst TE, Verbeeck H (2024) Evaluating airborne, mobile and terrestrial laser scanning for urban tree inventories: a case study in Ghent, Belgium. *Urban for Urban Green* 99:128428. <https://doi.org/10.1016/j.ufug.2024.128428>
- Delagrangé S, Jauvin C, Rochon P (2014) PypeTree: a tool for reconstructing tree perennial tissues from point clouds. *Sensors* 14(3):Article 3. <https://doi.org/10.3390/s140304271>
- Demol M, Wilkes P, Raunonen P, Krishna-Moorthy S, Calders K, Gielen B, Verbeeck H (2022) Volumetric overestimation of small branches in 3D reconstructions of *Fraxinus excelsior*. *Silva Fennica*. <https://doi.org/10.14214/sf.10550>
- Dettmann GT, MacFarlane DW (2019) Trans-species predictors of tree leaf mass. *Ecol Appl* 29(1):e01817. <https://doi.org/10.1002/eap.1817>
- Disney MI, Boni Vicari M, Burt A, Calders K, Lewis SL, Raunonen P, Wilkes P (2018) Weighing trees with lasers: advances, challenges and opportunities. *Interface Focus* 8(2):20170048. <https://doi.org/10.1098/rsfs.2017.0048>
- Du S, Lindenbergh R, Ledoux H, Stoter J, Nan L (2019) AdTree: accurate, detailed, and automatic modelling of laser-scanned trees. *Remote Sens* 11(18):Article 18. <https://doi.org/10.3390/rs11182074>
- Enquist BJ, Brown JH, West GB (1998) Allometric scaling of plant energetics and population density. *Nature* 395(6698):163–165. <https://doi.org/10.1038/25977>
- Enquist BJ, West GB, Charnov EL, Brown JH (1999) Allometric scaling of production and life-history variation in vascular plants. *Nature* 401(6756):907–911. <https://doi.org/10.1038/44819>
- Erker T, Wang L, Lorentz L, Stoltman A, Townsend PA (2019) A state-wide urban tree canopy mapping method. *Remote Sens Environ* 229:148–158. <https://doi.org/10.1016/j.rse.2019.03.037>
- Fan G, Nan L, Dong Y, Su X, Chen F (2020) AdQSM: a new method for estimating above-ground biomass from TLS point clouds. *Remote Sens* 12(18):Article 18. <https://doi.org/10.3390/rs12183089>
- Fernández-Sarría A, Velázquez-Martí B, Sajdak M, Martínez L, Estornell J (2013) Residual biomass calculation from individual tree architecture using terrestrial laser scanner and ground-level measurements. *Comput Electron Agric* 93:90–97. <https://doi.org/10.1016/j.compag.2013.01.012>
- Ferrarese J, Affleck D, Seielstad C (2015) Conifer crown profile models from terrestrial laser scanning. *Silva Fennica*. <https://doi.org/10.14214/sf.1106>
- Forrester DI, Tachauer IHH, Annighoefer P, Barbeito I, Pretzsch H, Ruiz-Peinado R, Stark H, Vacchiano G, Zlatanov T, Chakraborty T, Saha S, Sileshi GW (2017) Generalized biomass and leaf area allometric equations for European tree species incorporating stand structure, tree age and climate. *For Ecol Manag* 396:160–175. <https://doi.org/10.1016/j.foreco.2017.04.011>
- Franceschi E, Moser-Reischl A, Rahman MA, Pauleit S, Pretzsch H, Rötzer T (2022) Crown shapes of urban trees—their dependences on tree species, tree age and local environment, and effects on ecosystem services. *Forests* 13(5):748. <https://doi.org/10.3390/f13050748>
- Gonzalez De Tanago J, Lau A, Bartholomeus H, Herold M, Avitabile V, Raunonen P, Martius C, Goodman RC, Disney M, Manuri S, Burt A, Calders K (2018) Estimation of above-ground biomass of large tropical trees with terrestrial LiDAR. *Methods Ecol Evol* 9(2):223–234. <https://doi.org/10.1111/2041-210X.12904>
- Hackenberg J, Spiecker H, Calders K, Disney M, Raunonen P (2015) SimpleTree—an efficient open source tool to build tree models from TLS Clouds. *Forests* 6(11):Article 11. <https://doi.org/10.3390/f61114245>
- Henry M, Bombelli A, Trotta C, Alessandrini A, Birigazzi L, Sola G, Vieilledent G, Santenoise P, Longuetaud F, Valentini R, Picard N, Saint-André L (2013) GlobAllomeTree: international platform for tree allometric equations to support volume, biomass and carbon assessment. *iForest Biogeosci for* 6(6):326–330. <https://doi.org/10.3832/ifor0901-006>
- Kaasalainen S, Krooks A, Liski J, Raunonen P, Kaartinen H, Kaasalainen M, Puttonen E, Anttila K, Mäkipää R (2014) Change detection of tree biomass with terrestrial laser scanning and quantitative structure modelling. *Remote Sensing* 6(5):3906–3922. <https://doi.org/10.3390/rs6053906>
- Kükenbrink D, Gardi O, Morsdorf F, Thüring E, Schellenberger A, Mathys L (2021) Above-ground biomass references for urban trees from terrestrial laser scanning data. *Ann Bot* 128(6):709–724. <https://doi.org/10.1093/aob/mcab002>
- Larsen FK, Kristoffersen P (2002) *Tilia's* physical dimensions over time. *J Arboric* 28(5):209–214
- Lau A, Bentley LP, Martius C, Shenkin A, Bartholomeus H, Raunonen P, Malhi Y, Jackson T, Herold M (2018) Quantifying branch architecture of tropical trees using terrestrial LiDAR and 3D modelling. *Trees* 32(5):1219–1231. <https://doi.org/10.1007/s00468-018-1704-1>
- Liu Y, Guo J, Benes B, Deussen O, Zhang X, Huang H (2021) TreePartNet: neural decomposition of point clouds for 3D tree reconstruction. *ACM Trans Graph* 40(6):1–16. <https://doi.org/10.1145/3478513.3480486>
- López-López SF, Martínez-Trinidad T, Benavides-Meza H, García-Nieto M, De Los Santos-Posadas HM (2017) Non-destructive method for above-ground biomass estimation of *Fraxinus uhdei* (Wenz.) Lingelsh in an urban forest. *Urban for Urban Green* 24:62–70. <https://doi.org/10.1016/j.ufug.2017.03.025>
- MacFarlane DW (2010) Predicting branch to bole volume scaling relationships from varying centroids of tree bole volume. *Can J for Res* 40(12):2278–2289. <https://doi.org/10.1139/X10-168>
- MacFarlane DW (2015) A generalized tree component biomass model derived from principles of variable allometry. *For Ecol Manag* 354:43–55. <https://doi.org/10.1016/j.foreco.2015.06.038>
- Martin MP, Simmons C, Ashton MS (2016) Survival is not enough: the effects of microclimate on the growth and health of three common urban tree species in San Francisco, California. *Urban for Urban Green* 19:1–6. <https://doi.org/10.1016/j.ufug.2016.06.004>

- Martin-Guay M, Paquette A, Reich PB, Messier C (2020) Implications of contrasted above- and below-ground biomass responses in a diversity experiment with trees. *J Ecol* 108(2):405–414. <https://doi.org/10.1111/1365-2745.13265>
- Matthews G (1993) The carbon content of trees. Forestry Commission
- McHale MR, Burke IC, Lefsky MA, Peper PJ, McPherson EG (2009) Urban forest biomass estimates: is it important to use allometric relationships developed specifically for urban trees? *Urban Ecosyst* 12(1):95–113. <https://doi.org/10.1007/s11252-009-0081-3>
- McPherson EG, Van Doorn NS, Peper PJ (2016) Urban tree database and allometric equations (No. PSW-GTR-253; p. PSW-GTR-253). U.S. Department of Agriculture, Forest Service, Pacific Southwest Research Station. <https://doi.org/10.2737/PSW-GTR-253>
- Merganič J, Merganičová K, Konôpka B, Kučera M (2017) Country and regional carbon stock in forest cover—estimates based on the first cycle of the Czech National Forest Inventory data (2001–2004). *Cent Eur for J* 63(2–3):113–125. <https://doi.org/10.1515/forj-2017-0018>
- Metz J, Seidel D, Schall P, Scheffer D, Schulze E-D, Ammer C (2013) Crown modeling by terrestrial laser scanning as an approach to assess the effect of aboveground intra- and interspecific competition on tree growth. *For Ecol Manag* 310:275–288. <https://doi.org/10.1016/j.foreco.2013.08.014>
- Momo Takoudjou S, Ploton P, Sonké B, Hackenberg J, Griffon S, De Coligny F, Kamdem NG, Libalah M, Mofack GI, Le Moguédec G, Péliissier R, Barbier N (2018) Using terrestrial laser scanning data to estimate large tropical trees biomass and calibrate allometric models: a comparison with traditional destructive approach. *Methods Ecol Evol* 9(4):905–916. <https://doi.org/10.1111/2041-210X.12933>
- Montagu KD, Düttmer K, Barton CVM, Cowie AL (2005) Developing general allometric relationships for regional estimates of carbon sequestration—an example using *Eucalyptus pilularis* from seven contrasting sites. *For Ecol Manag* 204(1):115–129. <https://doi.org/10.1016/j.foreco.2004.09.003>
- LH München (2023) Statistisches Taschenbuch 2023. Statistisches Amt der Landeshauptstadt München. https://stadt.muenchen.de/dam/jcr%3Aaddaed0e-0914-4093-b46a-5a62acc9bf9/LHM-StatTB_2023_DS.pdf?utm_source=chatgpt.com
- Niklas KJ, Enquist BJ (2001) Invariant scaling relationships for interspecific plant biomass production rates and body size. *Proc Natl Acad Sci* 98(5):2922–2927. <https://doi.org/10.1073/pnas.041590298>
- Nowak DJ, Greenfield EJ (2020) The increase of impervious cover and decrease of tree cover within urban areas globally (2012–2017). *Urban for Urban Green* 49:126638. <https://doi.org/10.1016/j.ufug.2020.126638>
- Parmehr EG, Amati M, Taylor EJ, Livesley SJ (2016) Estimation of urban tree canopy cover using random point sampling and remote sensing methods. *Urban Forestry & Urban Greening* 20:160–171. <https://doi.org/10.1016/j.ufug.2016.08.011>
- Paul KI, Roxburgh SH, Chave J, England JR, Zerihun A, Specht A, Lewis T, Bennett LT, Baker TG, Adams MA, Huxtable D, Montagu KD, Falster DS, Feller M, Sochacki S, Ritson P, Bastin G, Bartle J, Wildy D, Sinclair J (2016) Testing the generality of above-ground biomass allometry across plant functional types at the continent scale. *Glob Change Biol* 22(6):2106–2124. <https://doi.org/10.1111/gcb.13201>
- Peper PJ, McPherson EG (1998) Comparison of five methods for estimating leaf area index of open-grown deciduous trees. *J Arboric* 24:98–111
- Phillips TH, Baker ME, Lautar K, Yesilonis I, Pavao-Zuckerman MA (2019) The capacity of urban forest patches to infiltrate stormwater is influenced by soil physical properties and soil moisture. *J Environ Manag* 246:11–18. <https://doi.org/10.1016/j.jenvman.2019.05.127>
- Picard N, Saint-André L, Henry M (2012) Manual for building tree volume and biomass allometric equations from field measurement to prediction. Food and Agriculture Organization of the United Nations (FAO)
- Pretzsch H (2009) Forest dynamics, growth, and yield: a review, analysis of the present state, and perspective. In: Pretzsch H (ed) *Forest dynamics, growth and yield*. Springer Berlin Heidelberg, pp 1–39. https://doi.org/10.1007/978-3-540-88307-4_1
- Pretzsch H (2010) Re-evaluation of allometry: state-of-the-art and perspective regarding individuals and stands of woody plants. In: Lüttge UE, Beyschlag W, Büdel B, Francis D (eds) *Progress in botany*, vol 71. Springer Berlin Heidelberg, pp 339–369. https://doi.org/10.1007/978-3-642-02167-1_13
- R Core Tea, v4. 3. 1 (2024) *R: A Language and Environment for Statistical Computing* [Computer software]. R Foundation for Statistical Computing, Vienna
- Radtke P, Walker D, Frank J, Weiskittel A, DeYoung C, MacFarlane D, Domke G, Woodall C, Coulston J, Westfall J (2017) Improved accuracy of aboveground biomass and carbon estimates for live trees in forests of the eastern United States. *Forestry* 90(1):32–46. <https://doi.org/10.1093/forestry/cpw047>
- Raunonen P, Kaasalainen M, Åkerblom M, Kaasalainen S, Kaartinen H, Vastaranta M, Holopainen M, Disney M, Lewis P (2013) Fast automatic precision tree models from terrestrial laser scanner data. *Remote Sens* 5(2):Article 2. <https://doi.org/10.3390/rs5020491>
- Roman LA, Scharenbroch BC, Östberg JPA, Mueller LS, Henning JG, Koeser AK, Sanders JR, Betz DR, Jordan RC (2017) Data quality in citizen science urban tree inventories. *Urban for Urban Green* 22:124–135. <https://doi.org/10.1016/j.ufug.2017.02.001>
- Rötzer T, Rahman MA, Moser-Reischl A, Pauleit S, Pretzsch H (2019) Process based simulation of tree growth and ecosystem services of urban trees under present and future climate conditions. *Sci Total Environ* 676:651–664. <https://doi.org/10.1016/j.scitotenv.2019.04.235>
- Rötzer T, Rahman MA, Pretzsch H, Pauleit S (2021) Leitfaden für Stadtbäume in Bayern: Handlungsempfehlungen aus dem Projekt Stadtbäume—Wachstum, Umweltleistungen und Klimawandel. (Hrsg.: Zentrum für Stadtnatur und Klimaanpassung., Ed.). Selbstverlag Bayerisches Staatsministerium für Umwelt und Verbraucherschutz, München. https://www.zsk.tum.de/fileadmin/w00bqp/www/PDFs/Leitfaeden/Anhang_Leitfaden_Stadtbaeume_komprimiert.pdf
- Seidel D, Leuschner C, Müller A, Krause B (2011) Crown plasticity in mixed forests—quantifying asymmetry as a measure of competition using terrestrial laser scanning. *For Ecol Manag* 261(11):2123–2132. <https://doi.org/10.1016/j.foreco.2011.03.008>
- Seiferling I, Naik N, Ratti C, Proulx R (2017) Green streets—quantifying and mapping urban trees with street-level imagery and computer vision. *Landsc Urban Plan* 165:93–101. <https://doi.org/10.1016/j.landurbplan.2017.05.010>
- Stoffberg GH, van Rooyen MW, van der Linde MJ, Groeneveld HT (2010) Carbon sequestration estimates of indigenous street trees in the City of Tshwane. *South Africa, Urban Forestry & Urban Greening* 9(1):9–14. <https://doi.org/10.1016/j.ufug.2009.09.004>
- Stovall AEL, Anderson-Teixeira KJ, Shugart HH (2018) Assessing terrestrial laser scanning for developing non-destructive biomass allometry. *For Ecol Manag* 427:217–229. <https://doi.org/10.1016/j.foreco.2018.06.004>
- Tarsha Kurdi F, Lewandowicz E, Gharineiat Z, Shan J (2024) Accurate calculation of upper biomass volume of single trees using matrixial representation of LiDAR data. *Remote Sens* 16(12):Article 12. <https://doi.org/10.3390/rs16122220>
- The MathWorks Inc. (2024) MathWorks—maker of MATLAB and Simulink. <https://www.mathworks.com/>

- Trochta J, Krůček M, Vrška T, Král K (2017) 3D Forest: an application for descriptions of three-dimensional forest structures using terrestrial LiDAR. *PLoS ONE* 12(5):e0176871. <https://doi.org/10.1371/journal.pone.0176871>
- Ucar Z, Bettinger P, Merry K, Akbulut R, Siry J (2018) Estimation of urban woody vegetation cover using multispectral imagery and LiDAR. *Urban Forestry & Urban Greening* 29:248–260. <https://doi.org/10.1016/j.ufug.2017.12.001>
- Vaz Monteiro M, Doick KJ, Handley P (2016) Allometric relationships for urban trees in Great Britain. *Urban for Urban Green* 19:223–236. <https://doi.org/10.1016/j.ufug.2016.07.009>
- Vejpustková M, Zahradník D, Čihák T, Šrámek V (2015) Models for predicting aboveground biomass of European beech (*Fagus sylvatica* L.) in the Czech Republic. *J for Sci* 61(2):45–54. <https://doi.org/10.17221/100/2014-JFS>
- Ver Planck NR, MacFarlane DW (2014) Modelling vertical allocation of tree stem and branch volume for hardwoods. *Forestry* 87(3):459–469. <https://doi.org/10.1093/forestry/cpu007>
- Ver Planck NR, MacFarlane DW (2015) A vertically integrated whole-tree biomass model. *Trees* 29(2):449–460. <https://doi.org/10.1007/s00468-014-1123-x>
- Weiner J (2004) Allocation, plasticity and allometry in plants. *Perspect Plant Ecol Evol Syst* 6(4):207–215. <https://doi.org/10.1078/1433-8319-00083>
- Weiskittel AR, MacFarlane DW, Radtke PJ, Affleck DLR, Temesgen H, Woodall CW, Westfall JA, Coulston JW (2015) A call to improve methods for estimating tree biomass for regional and national assessments. *J Forest* 113(4):414–424. <https://doi.org/10.5849/jof.14-091>
- Weller M (2021) Tree inventory data of Central European cities—studies on the composition and structure of urban tree populations and derivation of ecosystem services [Master thesis]. Technical University of Munich
- Wilkes P, Disney M, Vicari MB, Calders K, Burt A (2018) Estimating urban above ground biomass with multi-scale LiDAR. *Carbon Balance Manag* 13(1):10. <https://doi.org/10.1186/s13021-018-0098-0>
- Wu Z, Man W, Ren Y (2022) Influence of tree coverage and micro-topography on the thermal environment within and beyond a green space. *Agric for Meteorol* 316:108846. <https://doi.org/10.1016/j.agrformet.2022.108846>
- Xiao Q, McPherson EG, Ustin SL, Grismer ME (2000) A new approach to modeling tree rainfall interception *J Geophys Res: Atmos* 105(D23):29173–29188. <https://doi.org/10.1029/2000JD900343>
- Yang M, Zhou X, Liu Z, Li P, Tang J, Xie B, Peng C (2022) A review of general methods for quantifying and estimating urban trees and biomass. *Forests* 13(4):616. <https://doi.org/10.3390/f13040616>
- Yazdi H, Shu Q, Rötzer T, Petzold F, Ludwig F (2024) A multilayered urban tree dataset of point clouds, quantitative structure and graph models. *Sci Data* 11(1):28. <https://doi.org/10.1038/s41597-023-02873-x>
- Yazdi H, Chen X, Rötzer T, Parhizgar L, Pattnaik N, Ludwig F (2025) A 3D target-driven optimisation tool for tree planting location using temporal tree crown geometry development. <https://doi.org/10.21203/rs.3.rs-5521970/v1>
- Zianis D, Muukkonen P, Mäkipää R, Mencuccini M (2005) Biomass and stem volume equations for tree species in Europe. *Silva Fennica Monogr* 2005(4):1–63. <https://doi.org/10.14214/sf.sfm4>

Publisher's Note Springer Nature remains neutral with regard to jurisdictional claims in published maps and institutional affiliations.